Bone mimetics: a composite of hydroxyapatite and calcium dodecylphosphate lamellar phase

Geoffrey A. Ozin,*[a] Natalia Varaksa,[a] Neil Coombs,[b] John E. Davies,[c] Douglas D. Perovic[d] and Martine Ziliox[e]

[a] *Materials Chemistry Research Group, Lash Miller Chemical Laboratories, University of Toronto, 80 St. George Street, Toronto, Ontario, Canada M5S 3H6*
[b] *Imagetek Analytical Imaging, 32 Manning Av., Toronto, Ontario, Canada M6J 2K4*
[c] *Center of Biomaterials, University of Toronto, 170 College Street, Toronto, Ontario, Canada M5S 1A1*
[d] *Department of Metallurgy and Material Science, University of Toronto, 184 College Street, Toronto, Ontario, Canada M5S 3E4*
[e] *Bruker Instruments Company, Fortune Drive, Manning Park, Billerica, MA 01821, USA*

The synthesis of composites based upon mineral and organic constituents is of importance for the development of materials for biomedical applications, such as bone replacement, augmentation and repair. Herein we describe a biologically inspired inorganic materials chemistry approach to bone mimetics. The synthetic strategy is based upon the surfactant-templated cooperative assembly of a composite that is composed of a calcium dodecylphosphate lamellar phase (CaDDP) and a calcium hydroxyphosphate (CaP) mineral phase. The measured properties of the chemically formed composite suggest that it is distinct from simple physical mixtures of the CaDDP and CaP components. A key difference is the generation of biologically important hydrogenphosphate located at the interface between the CaDDP and CaP phases only in the chemically formed composite. The synthesis of the composite is considered to involve the synergistic interaction of CaDDP and CaP, possibly aided by interfacial complementarity of charge and geometry. CaDDP is chemically stable and non-toxic, rendering the composite potentially useful for biomedical applications.

Composite materials have gained widespread recognition in different fields of application.[1] Multicomponent materials embrace a large class of compositions and constituents, from fibre-reinforced composites to bioactive ceramic–polymer composites. All of them have certain features in common, including the following: (*a*) they contain two or more distinct but closely related phases, which may be continuous or discontinuous; (*b*) these phases are related to each other depending upon the adhesive mechanism at the interface of two or more phases;[2] (*c*) the properties of composites are distinct from those of the individual components acting alone. The nature of the interface often dictates the properties of the composite, and the superior characteristics of composites are usually unattainable by the individual constituents.

One of the most striking examples of a naturally occurring composite is bone. At the molecular level bone is a two-phase composite. The main constituents of bone are a collagen matrix and assembled crystals of calcium phosphate, mainly in the form of carbonate apatite or carbonate fluorapatite. The needle-like or plate-like crystals are oriented with their long axes parallel to the direction of collagen fibrils, and they are located within and around the collagen fibrils. The chemical composition, the structure of calcium phosphate in bone, and its possible precursors are still debated. Attention is drawn to the presence of monohydrogenphosphate, HPO_4^{2-}, groups in the apatitic structure because of their importance in the bone physiology, turnover and remodelling. The HPO_4^{2-} groups in bone samples have been detected by different methods including chemical analysis,[3] (FTIR)[4] and ^{31}P NMR spectroscopy.[5] Aside from the arrangement of mineral crystals within collagen fibrils a very important aspect of the relationship between the phases is the interaction of the mineral crystals with the bone organic phase, mainly collagen. There are several contradictory models described in the structural biomaterials literature.[6,7] The model of widest acceptance is that 75% of hydroxyapatite is located in the gaps within collagen fibrils, and some of it is not crystalline. Moreover, not all of the mineral constituents of bone intimately interact with collagen. However, it should be remembered that the body fluid and calcifying tissues contain a large variety of biological chemicals including bone-specific proteins, which are phosphorylated amino acid residues (phosphoproteins) and phospholipids. All of them play a crucial role in the nucleation of calcium phosphate crystals, providing the surface and specific nucleation sites for biological mineralization. These features of the calcification process offer numerous opportunities for the preparation of bone-like synthetic materials. At a higher level of structural organization, the bone includes cells (osteocytes), enclosed in small cavities of the tissue, and blood vessels. At this level of hierarchy, the bone can no longer be considered as merely a composite material. Therefore, the interaction of bone-like synthetic materials with living tissue does not boil down to the simple chemical compatibility between them, although such a unity is a necessary condition for tissue attachment and response. The formation of the crystalline phase of bone is controlled by many complex biological processes, and the tissue response at the implant–bone interface is hard to predict. That is the reason why amongst the many promising implanted materials only a few are clinically successful. However, even the best materials do not meet all of the necessary pre-requisites, such as biocompatibility, strength, ductility, long-term performance and mechanical compatibility. The main types of implanted materials used at the present time are the following: metals (stainless steel, cobalt alloys, titanium alloys), ceramics and polymers (polyethylene, PMMA). Combinations of different types of materials allow the production of composite bone and tissue analogues. The most known examples of this type are collagen–plastic and hydroxyapatite–polymer composites.[8]

In this article we describe the surfactant-based synthesis of a composite that is comprised of a calcium dodecylphosphate (CaDDP) lamellar phase and a calcium phosphate (CaP) mineral phase. The measured properties of the composite are found to be distinct from those of the individual components as well as simple physical mixtures thereof. A model is proposed for the composite that invokes co-assembly of the CaDDP and CaP components.

Experimental

Preparation of a CaDDP lamellar and a CaDDP/CaP composite phase

Mono-*n*-dodecylphosphate, or phosphoric acid monododecyl ester (Lancaster), insoluble in water, was transformed to the water-soluble form, potassium dodecylphosphate (K_2DDP), by neutralization of the acid form with a solution of potassium hydroxide (BDH). The concentration of K_2DDP varied from 3 to 5%. The addition of $CaCl_2$ (Fisher) solution resulted in an immediate precipitation of flake-like coarse particles of calcium dodecylphosphate, CaDDP. This precipitate was washed with water, separated by vacuum filtration and air-dried at ambient temperature. The CaDDP powder was dispersed in a 0.1 M aqueous solution of dibasic potassium phosphate, K_2HPO_4 (Fisher), the pH of the mixture was maintained at 8–9 by a 0.1 M solution of phosphoric acid (Mallinckrodt, 85%). The 0.1 M aqueous solution of $CaCl_2$ was added slowly (dropwise) to this dispersed system for the nucleation of calcium phosphate crystals. This mixture was aged at 80 °C for 14 days. The obtained precipitate was washed with water, filtered and air-dried at room temperature. Powder X-ray diffraction, ^{31}P CP MAS NMR spectroscopy, and field emission transmission electron microscopy with quantitative energy dispersive X-ray analysis together show that the mineral phase synthesized according to the above procedure is calcium hydroxyphosphate with a Ca : P ratio of 1.67 and that the lamellar phase is calcium dodecylphosphate (see below for details).

Instrumentation

Transmission electron microscopy (TEM) and scanning transmission electron microscopy (STEM) were performed on a JEOL 2010F field-emission electron microscope operating at 200 kV with minimum probe diameter of *ca.* 0.4 nm. The following analytical techniques were employed: high-resolution phase contrast imaging (through focal series), selected area and nanoprobe electron diffraction, energy dispersive X-ray spectroscopy (EDX) and electron energy-loss spectroscopy (EELS). FTIR spectra were obtained in the range 4000–400 cm^{-1} using a Nicolet 2SX IR spectrometer. The resolution was 2 cm^{-1}, and the number of scans was 30. Ground samples were dispersed in KBr and pressed into discs [concentration 1 mg 300 mg^{-1}]. Thermogravimetry (TG) was carried out on a Perkin-Elmer TAS 7 thermal analyser. The sample masses ranged from 9 to 24 mg, the speed of heating was 5 °C min^{-1}, the data were recorded under nitrogen, and heating was up to 600 °C. Powder X-ray diffraction (PXRD) data of materials, packed in a standard sample holder, were obtained on a Siemens D5000 powder diffractometer using Cu-Kα radiation and a solid-state (Kevex) detector. For routine scans the counting time per step and the step size were 1.5 s and 0.02°, respectively. The ^{1}H and ^{31}P MAS NMR spectra were recorded with a 400 MHz Bruker DSX-400 spectrometer. The single pulse technique was applied, the recycle delay was 4 s, and the spinning rate of the rotors was 10 kHz. The spectra were taken with high-power proton decoupling. Chemical shift values are given with respect to TMS for protons and $(NH_4)H_2PO_4$ for ^{31}P. The cross-polarization (CP) MAS experiments were carried out for the purpose of enhancing the relative intensity of phosphate groups in the CaDDP and CaP phases, with nearby protons. The cross-polarization contact time was 2 ms, recycle delay 4 s. All powdered samples (hydrated and dehydrated at 120 °C) were tightly packed into 7 mm rotors.

Results

Electron microscopy

Fig. 1(A) and (B) depict the high-resolution field emission transmission electron microscope (HR-FETEM) images of the lamellar CaDDP phase. The dark areas representing high electron density regions correspond to the phosphate head groups of the surfactant, electrostatically bound to calcium(II) ions. The intermediate light areas depict regions occupied by the hydrocarbon tails of the surfactant. The interlayer distance is *ca.* 29 Å, which correlates with the overlap of surfactant tails and/or their tilt with respect to the normal, and is consistent with the PXRD d_{001}-spacing of the CaDDP phase, see later. From the energy dispersive X-ray fluorescence analysis (EDX) data, the molar ratio of calcium to phosphate is unity, which is consistent with the charge-balance requirements and the stoichiometry $CH_3(CH_2)_{11}OPO_3Ca$ for the CaDDP lamellar phase.

Fig. 2(A) and (B) show TEM images of the composite material. A number of crystals of calcium phosphate are oriented with respect to the CaDDP layers. The long axes of the crystals are aligned parallel to the direction of the layers. Other crystals, far apart from the lamellae, are randomly distributed in the void spaces between the lamellar aggregates. The average crystal size falls in the range of (400–800 Å) × (30–50 Å). Nanoelectron diffraction patterns of the mineral phase recorded for a large number of crystals, shows them to be highly crystalline and apatitic while quantitative EDX analysis establishes them to have a Ca : P ratio of 1.67. This is confirmed by HR-FETEM lattice imaging of the apatite crystals, which demonstrates that the long direction is the *c*-axis and that they are essentially devoid of octacalcium phosphate intergrowths.

FTIR spectra

The FTIR spectra, Fig. 3, of CaDDP and the final organic–inorganic composite exhibit two characteristic absorption bands[9,10] [750–770 cm^{-1} for the (P—O)—C bond and 950–1015 cm^{-1} for the P—(O—C) bond]. The overlap of high-wavenumber bands (950–1015 cm^{-1}) due to the presence of inorganic calcium phosphate prevents unequivocal identification of these bands, which can belong to several kinds of phosphate species. The low-wavenumber bands (750–770 cm^{-1}) are sufficiently prominent in these two above-mentioned phases (CaDDP and CaDDP/CaP composite) and suggest the presence of an unhydrolysed (P—O)—C bond.[9,11–14] The PO_4 bands at 1200–960 cm^{-1} (stretch) and 650–500 cm^{-1} (bend) are clear. The absence of absorption bands at 861, 917, 1193 and 1295 cm^{-1}, assigned to P—OH stretching and in-plane bending modes of $HPO_4{}^{2-}$ groups of octacalcium phosphate,[15] indicates that this phase of calcium phosphate, the structure of which is very close to that of hydroxyapatite, does not form in the synthesis of composite material. The transformation of the broad water band at 3600–3000 cm^{-1} for CaDDP to a sharp bend at *ca.* 3600 cm^{-1} for the CaDDP/CaP composite, suggests that the latter loses some interlamellar water molecules from the CaDDP phase. There appear to be at least two kinds of water intercalated in the lamellar space of the CaDDP phase, as seen from the TG (see later) of the hydrated and dehydrated materials.

Powder X-ray diffraction analysis

A representative powder X-ray diffraction pattern obtained from the CaDDP phase is illustrated in Fig. 4. The low-angle region shows the (001) reflections with a *d*-spacing of 29 Å, while the high-angle region is devoid of calcium phosphate reflections. This is consistent with the proposal that PO—C bond hydrolysis is negligible, if it is occurring at all. The

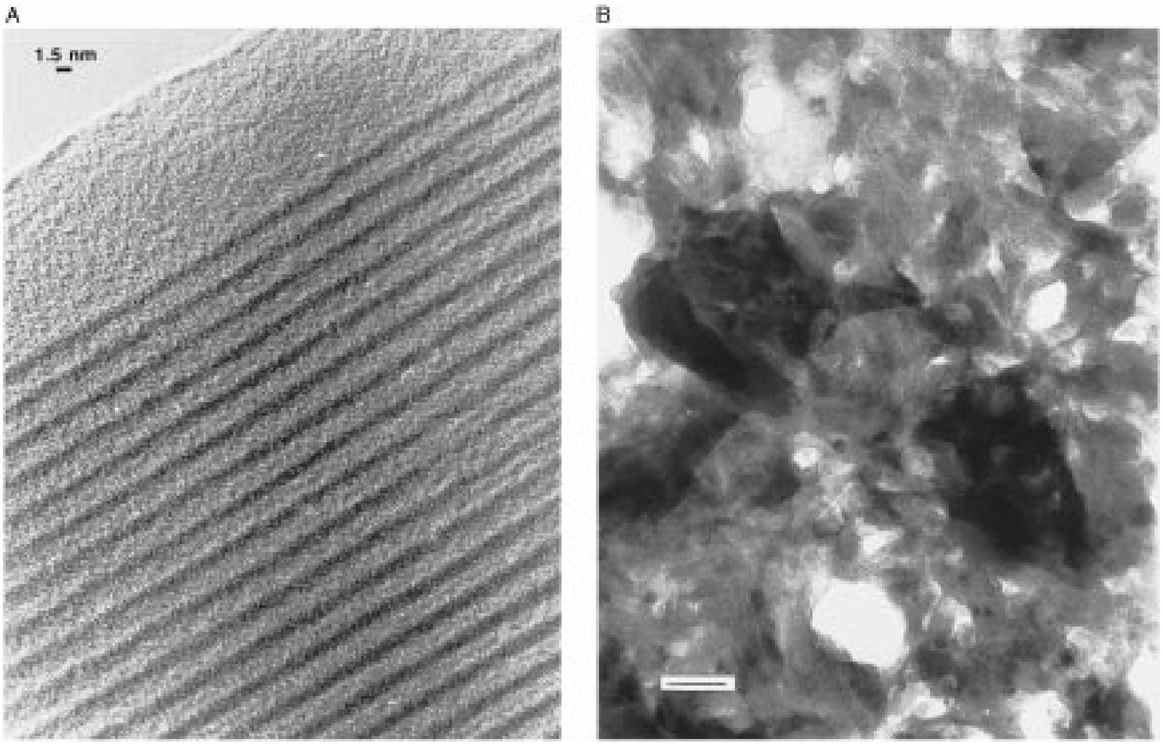

Fig. 1 TEM images of CaDDP, calcium dodecylphosphate lamellae (A scale bar = 1.5 nm; B scale bar = 100 nm)

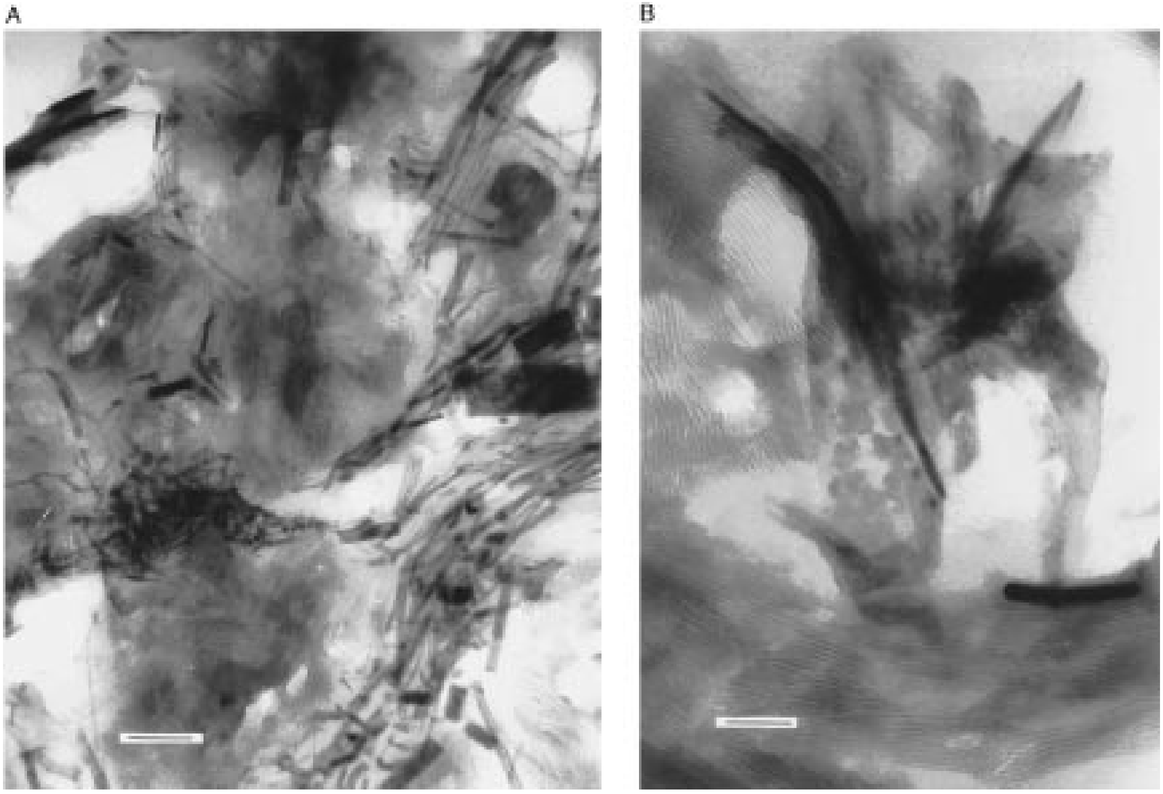

Fig. 2 TEM images of chemical composite CaDDP/CaP material (A scale bar = 200 nm; B scale bar = 50 nm)

PXRD pattern of the CaDDP/CaP composite displays low-angle (001) reflections characteristic of the CaDDP lamellar phase (*d*-spacing 35 Å) and high-angle reflections typical of the CaP hydroxyapatite phase,[16] Fig. 4. The broadness of the diffraction peaks of the calcium phosphate component relative to that of pure crystalline hydroxyapatite implies small particle size and/or lower crystallinity (lattice imperfections, crystal defects). Small changes are observed in the d_{001}-spacing on passing from the CaDDP to the CaDDP/CaP phase, which appear to correlate with variations in the interlamellar water content, and are likely associated with alterations in the surfactant bilayer tilt-angle and/or interlayer distance.

Thermogravimetry

Thermogravimetry (TG) results for the pure CaDDP material and the composite CaDDP/CaP phase are depicted in Fig. 5. The two main mass losses in the region around 100 °C likely

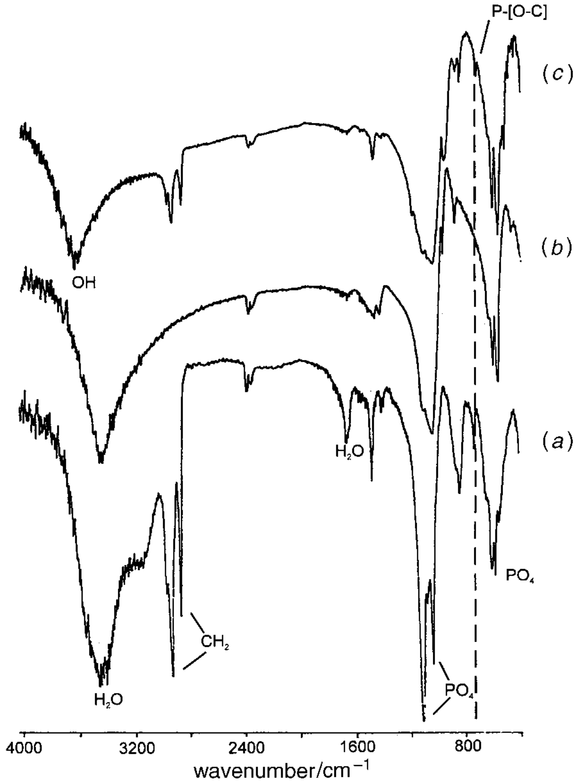

Fig. 3 IR spectra of pure CaDDP, calcium dodecylphosphate lamellae (*a*); CaP, hydroxyapatite (*b*); and CaDDP/CaP composite material (*c*)

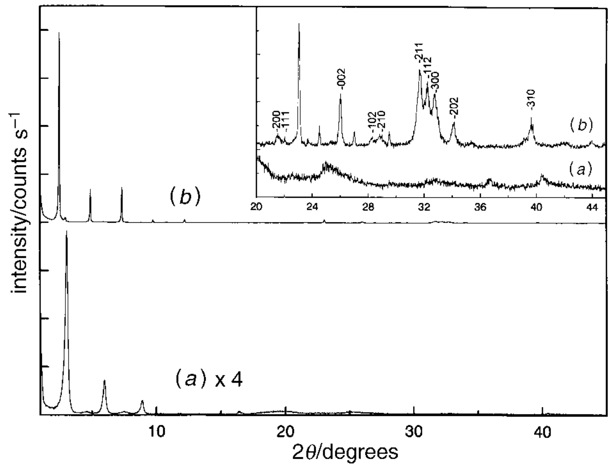

Fig. 4 PXRD patterns of CaDDP, calcium dodecylphosphate lamellae (*a*), and chemical composite CaDDP/CaP material (*b*). Insert shows a scale expansion of the high-angle region.

correspond to physisorbed and/or chemisorbed water contained in the interlamellar regions of the CaDDP phase. The structure of the materials is maintained intact on removing the intercalated water (PXRD). The thermal transitions around 250–350 °C correspond to the loss/decomposition of the interlamellar phosphate ester, concurrent with the collapse of the lamellae, as seen by the disappearance of the low-angle PXRD reflections that correspond to the interlayer *d*-spacing.

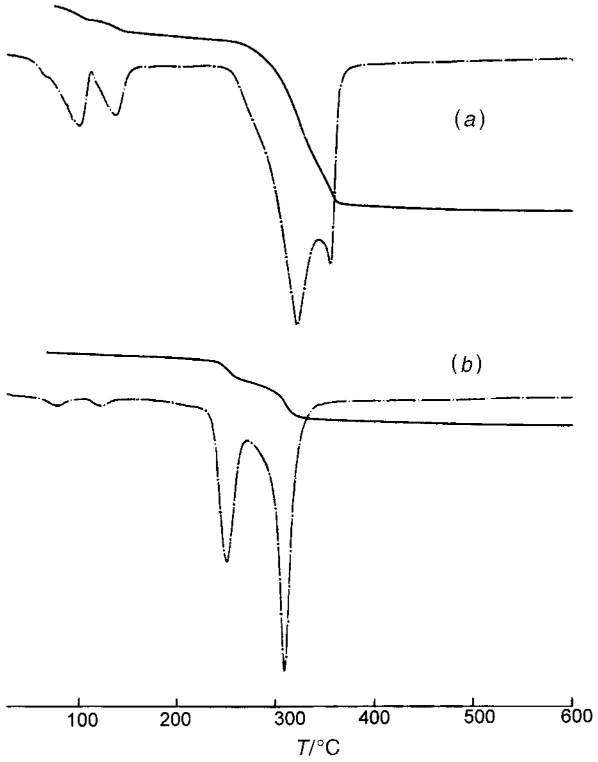

Fig. 5 Thermograms of the CaDDP calcium dodecylphosphate lamellae (*a*) and the chemical composite CaDDP/CaP material (*b*), showing the loss of mass (—) and the first derivative of this parameter (–·–)

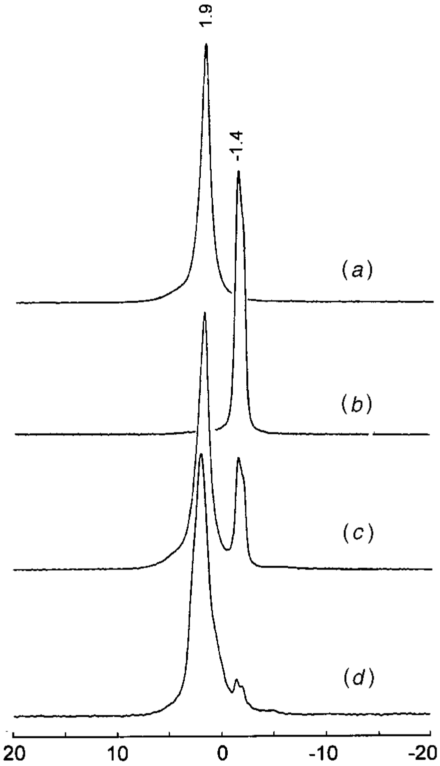

Fig. 6 ^{31}P MAS NMR spectra of CaP calcium phosphate (*a*), CaDDP calcium dodecylphosphate lamellae (*b*), their physical CaDDP/CaP mixture (*c*), and chemical CaDDP/CaP composite (*d*)

NMR spectroscopy

The ^{31}P MAS NMR spectrum of the pure mineral phase, Fig. 6, shows a single resonance at 1.9 ppm (2.8 ppm for OHAp, 1.4 ppm for brushite, 3.4, −0.1 ppm for OCP,[17] or 3.3, 2.2, −0.2 ppm for OCP)[18]. No cross-polarization enhancement is observed on this signal which is consistent with the lack of nearby protons in the CaP lattice. The ^{1}H MAS NMR spectrum, Fig. 7, on the other hand, reveals two peaks (−0.2, 4.9 ppm) likely originating from hydroxy groups (0.2 ppm) and surface adsorbed water (5.5 ppm).[19] The high field shift of the hydroxy group resonance in the composite (−0.2 ppm) may be due to weaker hydrogen bonding between the OH groups

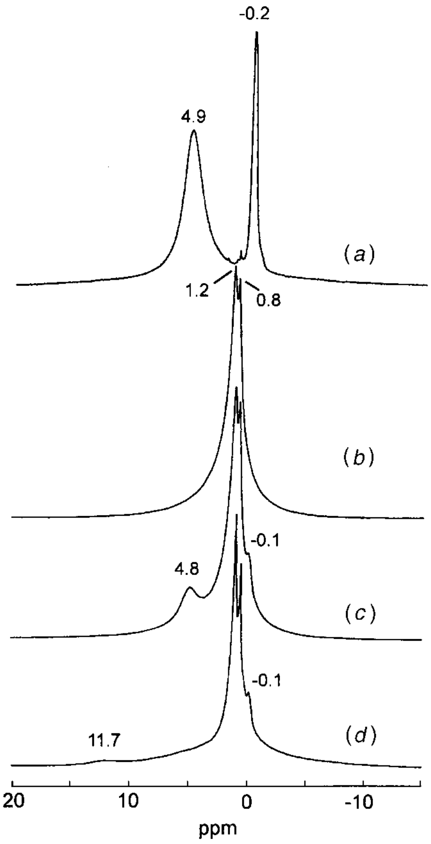

Fig. 7 Proton MAS NMR spectra of CaP calcium phosphate (*a*), CaDDP calcium dodecylphosphate lamellae (*b*), their physical CaDDP/CaP mixture (*c*), and chemical CaDDP/CaP composite (*d*)

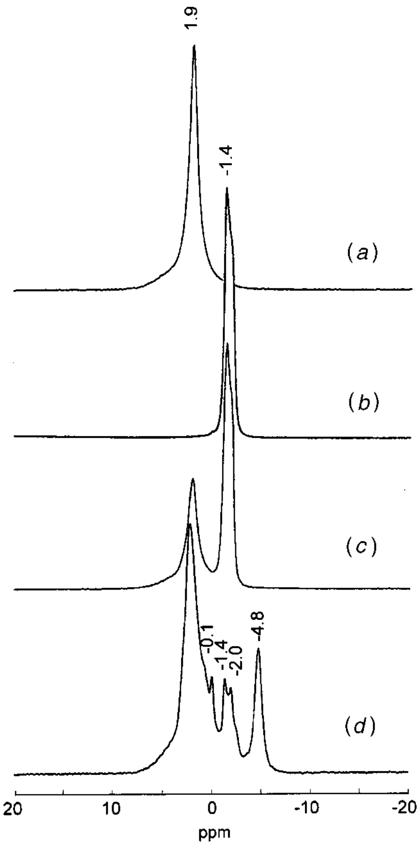

Fig. 8 ^{31}P CP MAS NMR spectra of CaP calcium phosphate (*a*), CaDDP calcium dodecylphosphate lamellae (*b*), their physical CaDDP/CaP mixture (*c*), and chemical CaDDP/CaP composite (*d*)

in the hydroxyapatite-like structure of the mineral phase. The ^{31}P MAS NMR spectrum of CaDDP shows a split resonance around -1.4 ppm which likely corresponds to two distinct phosphate sites in the lamellae. The absence of cross-polarization enhancement confirms that the phosphate head groups are not protonated but instead charge-balance the interlamellar Ca^{2+} ion, consistent with the stoichiometry, $CH_3(CH_2)_{11}OPO_3Ca$ from HR-FETEM–EDX (see above). The physical mixture of CaDDP/CaP displays ^{31}P MAS and CP MAS NMR spectra that correspond well to a simple superposition of the two phases, Fig. 6 and 8. The distinctive feature of the CP MAS spectrum is the enhanced intensity of the CaDDP peak relative to that of the inorganic calcium phosphate. Such an enhancement of the magnetization of phosphorus nuclear spins could arise from non-directly attached protons, such as the α-methylene protons of the hydrocarbon tail or interlamellar water. In this case, no changes in the configuration of the phosphate head group and the phosphorus nuclei shielding occur, and therefore, the chemical shift remains unchanged.

By contrast, the ^{31}P MAS and CP MAS NMR spectra of the CaDDP/CaP composite is notably distinct to those of the physical mixture. In particular, the CaP region shows a new upfield signal around -0.06 ppm, which can be reasonably ascribed to a protonated phosphate in the mineral phase. In addition, the CaDDP region shows a new upfield signal near -4.8 ppm. Two factors can give rise to the larger shielding effect on the phosphorus nucleus: the formation of a protonated phosphate head group and changes in the O—P—O bond angle.[20] In both cases, the cross-polarization technique enhances the appropriate signal intensities, provided that nearby (or remote) protons contribute to the magnetization transfer to phosphorus nuclei. It is noteworthy that the observed CP enhancement of the unique phosphorus nuclei remains essentially invariant to the removal of interlayer water. This implies that the magnetization transfer stems mainly from protonated phosphate head groups most likely located in the interfacial region between the CDDP andd CaP phases.

Discussion

The observed and reproducible changes in the PXRD *d*-spacings, IR band positions, TG thermal transition temperatures, NMR chemical shifts and their cross-polarization behaviour, indicate that the composite is distinct from the pure CDDP phase and the physical mixture CDDP/CaP. The results suggest that the composite material forms from the co-assembly of the lamellar CaDDP and inorganic CaP phases. The precursor for the organic constituent of the composite is the water-soluble potassium dodecylphosphate, K_2DDP, which self-assembles to a lamellar structure. This phosphate ester surfactant has an affinity for Ca^{2+}. Thus, the addition of $CaCl_2$ or $Ca(NO_3)_2$ solution to the K_2DDP phase induces the precipitation of the CaDDP phase having a 29 Å interlamellar distance. The phosphate ester surfactant does not undergo hydrolysis under these experimental conditions. The surface of the CaDDP serves as a substrate for the nucleation and growth of calcium phosphate crystals. In order to create a larger surface, the CaDDP aggregates were peptized in the appropriate electrolyte solution (dibasic potassium phosphate). The nucleation and growth of calcium phosphate occurs upon the addition of a calcium chloride solution. The deposited mineral phase appears to be different from calcium phosphate, obtained without the CaDDP phase under the same conditions. Protonated HPO_4^{2-} phosphate groups appear in the composite, CaDDP/CaP. The location of the HPO_4^{2-} groups in the composite phase is not entirely clear, but their emergence is induced by the interaction of CaP with the CaDDP phase, likely followed by the formation of a calcium–surfactant–phosphate complex at the interface. Some of the phosphate

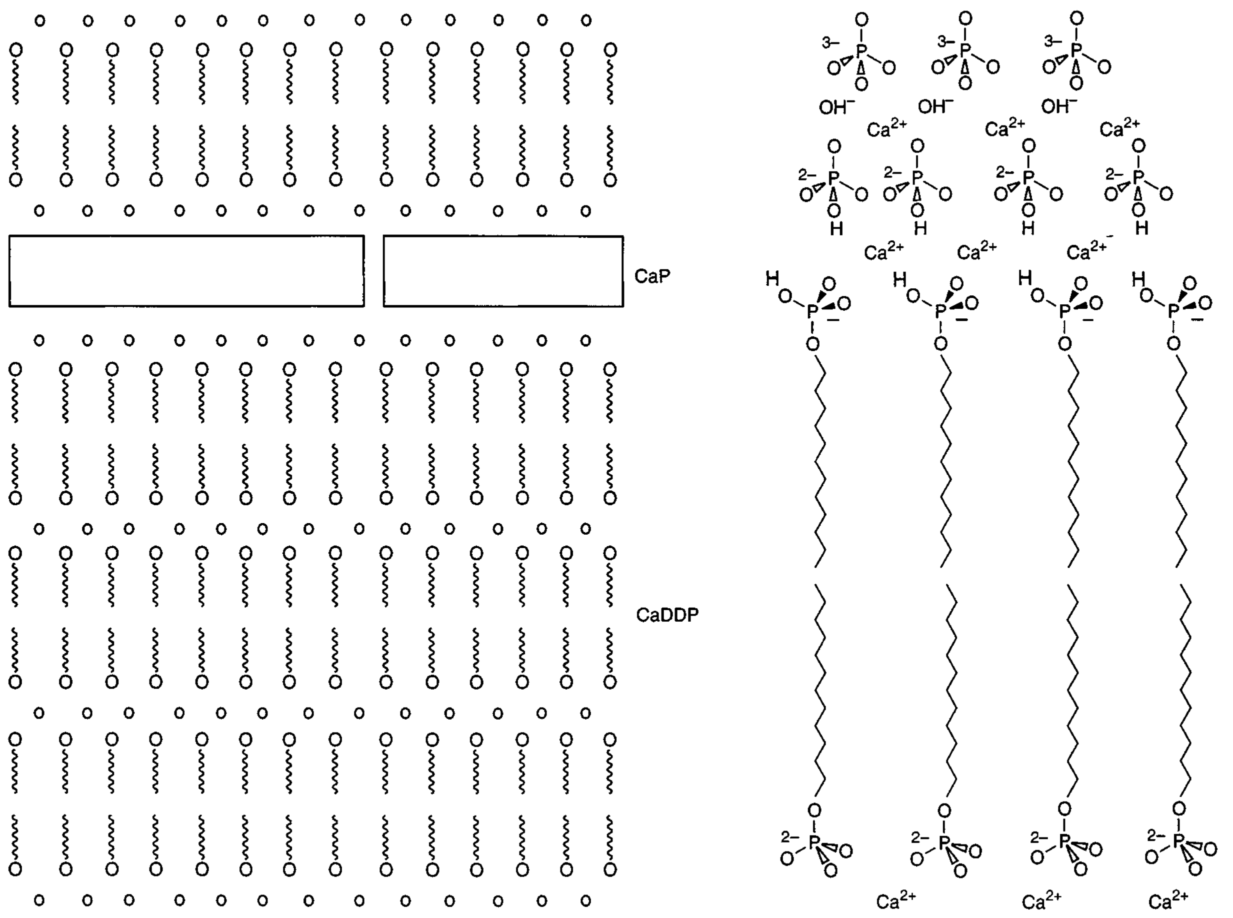

Fig. 9 Illustration of the proposed model of the chemical composite of hydroxyapatite (CaP) and calcium dodecylphosphate (CaDDP) lamellar phase (left), emphasizing the location of the biologically significant charge balancing hydrogenphosphate at the interface between the two components (right)

head groups of the CaDDP phase comprising the composite material are found, from the NMR studies, to be distinct from those of pure CaDDP. Judging by the upfield shift and a large CP MAS ^{31}P enhancement in comparison with the peak at -1.4 ppm, there are protonated phosphate groups in the lamellae. They also likely contribute to the formation of the interfacial calcium–surfactant–phosphate complex bridged with Ca^{2+} ions, which is strongly supported by ^{31}P NMR data, as illustrated in Fig. 9. The TEM image, Fig. 2(B), shows close contact between some of the CaDDP and CaP crystals. Other crystals join up to form larger agglomerates. The presence of HPO_4^{2-} in the mineral phase is considered to be very important from the biological point of view. It is known that bone contains some number of protonated phosphate ions, which can play a crucial role in the bone metabolism and the interaction between the organic and inorganic constituents of bone.

Conclusions

It seems that the chemically formed composite that is synthesized by the surfactant-templated cooperative assembly of a calcium dodecylphosphate lamellar phase (CaDDP) and a calcium hydroxyphosphate (CaP) mineral phase is distinct from pure CaDDP as well as a physical mixture of CaDDP and CaP. A key difference is the generation of biologically important hydrogenphosphate located at the interface between the CaDDP and CaP phases only in the chemically formed composite. Insertion of bioactive guest molecules into the hydrophobic bilayer of the CaDDP host, incorporation of the CaDDP/CaP into polymer, metal and bioceramic matrices, and the adsorption/self-assembly of the composite on metal or metal oxide surfaces, are ways to expand the potential utility of the composite.

This work was generously funded by the Interdisciplinary Section of the Collaborative Research Programme of the Natural Sciences and Engineering Research Council of Canada, NSERC. University of Toronto principal investigators of the project 'Calcium Phosphate Composite Mesostructures as Bone Analogue Materials' are: Dr. John E. Davies, Dr. Geoffrey A. Ozin, Dr. Peter M. Macdonald and Dr. Douglas D. Perovic. Discussions with Dr. Alex Kuperman proved to be most valuable. The technical assistance of Ms. Ivana Soten and Ms. Deepa Khushalani is deeply appreciated.

References

1 *Hierarchical Structures in Biology as a Guide for New Materials Technology*, National Materials Advisory Board, National Academy Press, Washington DC, 1994.
2 D. Hull, *An Introduction to Composite Materials*, Cambridge University Press, 1981.
3 M. J. Dallemagne and L. J. Richelle, in *Biological Mineralization*, ed. I. Zipkin, Wiley, New York, 1973.
4 C. Rey, M. Shimizu, B. Collins and M. J. Glimcher, *Calcif. Tissue Int.*, 1990, **46**, 384.
5 W. P. Aue, A. H. Roufosse, M. J. Glimcher and R. G. Griffin, *Biochemistry*, 1984, **23**, 6110.
6 J. Vincent, *Structural Biomaterials*, Princeton University Press, 1990.
7 *Tissue Engineering*, *MRS Bull.*, 1996, **21**, 18.
8 J. Emsley and D. Hall, *The Chemistry of Phosphorus*, Harper & Row, 1976.
9 M. Subirade and A. Lebugle, *Ann. Chim. Fr.*, 1991, **16**, 41.

10 C. Rey, M. Shimizu, B. Collins and M. J. Glimcher, *Calcif. Tissue Int.*, 1991, **49**, 383.
11 C. A. Bunton, D. R. Llewellyn, K. G. Oldham and C. A. Vernon, *J. Chem. Soc.*, 1958, **3**, 3574.
12 W. W. Butcher and F. H. Westheimer, *J. Am. Chem. Soc.*, 1955, **77**, 2420.
13 M. Okazaki, *Biomaterials*, 1991, **12**, 46.
14 M. Okazaki and M. Hattori, *Biomaterials*, 1989, **10**, 126.
15 B. O. Fowler, M. Markovic and W. E. Brown, *Chem Mater.*, 1993, **5**, 1417.
16 *Structure and Chemistry of the Apatites and Other Calcium Orthophosphates*, ed. J. C. Elliott, Elsevier Science, Amsterdam, 1994.
17 W. P. Rothwell, J. S. Waugh and J. P. Yesinowski, *J. Am. Chem. Soc.*, 1980, **102**, 2637.
18 J. L. Miquel, L. Facchini, A. P. Legrand, X. Marchandise, P. Lecouffe, M. Chanavaz, M. Donazzan, C. Rey and J. Lemaitre, *Clin. Mater.*, 1990, **5**, 115.
19 J. P. Yesinowski and H. Eckert, *J. Am. Chem. Soc.*, 1987, **109**, 6274.
20 D. G. Gorenstein, *J. Am. Chem. Soc.*, 1975, **97**, 898.

Paper 7/02416I; *Received* 9*th April*, 1997